

# Spectroscopic Determination of Impact Sensitivities of Explosives

K. L. McNesby\*

U.S. Army Research Laboratory, Aberdeen Proving Ground, Maryland 21005-5066

C. S. Coffey

Naval Surface Warfare Center, Silver Spring, Maryland 20903-5000

Received: June 17, 1996; In Final Form: October 18, 1996<sup>®</sup>

A simple theory is developed which predicts impact sensitivities in crystalline explosives from vibrational spectra measured at room temperature. The theory uses Raman spectra of energetic materials to construct vibrational energy level diagrams, which are then used as input for a model designed to calculate the rate of energy transfer from phonon and near-phonon vibrational energy levels to higher energy vibrational levels. Energy transfer rates are determined using Fermi's Golden Rule and results from simple theories of near-resonant energy transfer. The application of the theory and model, using Raman spectra of seven different neat explosive samples, gives results in good agreement with results of drop weight impact tests.

## Introduction

One of the simplest and oldest tests used to determine relative sensitivities of explosives and propellants is the drop weight impact test.<sup>1</sup> Although there are many variations of the test, in general, all such tests involve dropping a weight from various heights onto a small amount of explosive or propellant and determining the minimum drop height that causes the material to react. Typical experimental parameters use tens of milligrams of explosive or propellant, and drop a several kilogram weight from several to hundreds of centimeters in height.<sup>2</sup> Results are reported in terms of Go–No Go, where a Go may range from an explosion to a smoldering deflagration. An example of a typical drop weight test apparatus is shown in Figure 1.

Results from an impact test designed to measure the energy transferred to the sample show that for sensitive explosives initiation occurs early in the impact event,<sup>2</sup> when there is a relatively small decrease in the velocity of the impactor. Typically, results show that ignition of a 50 mg explosive sample occurs when the change in kinetic energy of the impactor ( $V_0 > 10$  m/s) is on the order of a few joules and that initiation occurs from several to tens of microseconds after the impactor comes in contact with the sample,<sup>2</sup> when the velocity of the impactor has decreased by just a few percent (see Figure 2).

Assuming a heat capacity,<sup>3</sup>  $C_p$ , of the sample at room temperature similar to the explosive RDX (0.3 cal/g K), and uniform distribution of 2 J of energy throughout a 50 mg sample, the change in sample temperature,  $\Delta T = \Delta E/C_p$ , for the typical test just described, is approximately 31 K. Since this temperature rise is insufficient to initiate reaction in practically all energetic materials, the kinetic energy of the impactor, for a Go event, must be localized over a small fraction of the entire sample. From this it follows that for materials of differing impact sensitivity, the volume of material into which the impact energy is distributed determines the impact sensitivity.

Some current theories of impact sensitivity<sup>4</sup> postulate that initiation is due to energy dissipation and localization that takes place during plastic deformation, and the ability of the material to shear along certain axes.<sup>5</sup> For these theories, rates of intramolecular energy transfer within the molecules making up the molecular crystal are secondary, since the volume into which

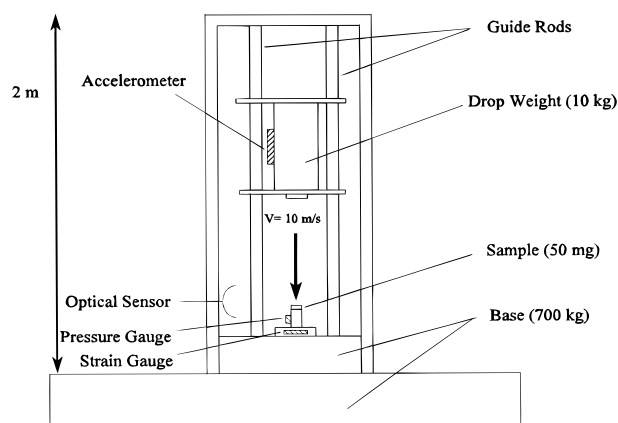


Figure 1. Example of a typical drop-weight test apparatus.

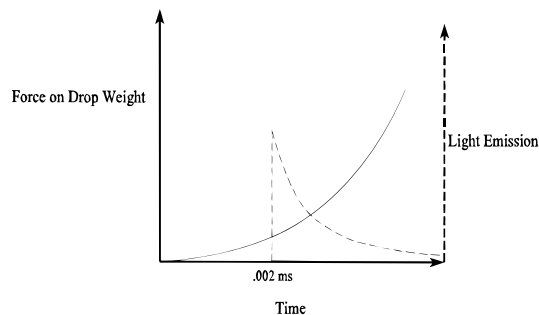
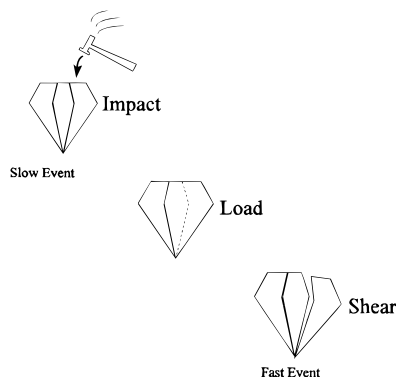


Figure 2. Typical results of an energy-to-ignition test, showing initiation occurring early in the impact event.

the impact energy is deposited is sufficiently small that the temperature rise of the material within the perturbed volume is several times the decomposition temperature. If low-energy impact initiation is such a thermal process, a measurement of the ability of a series of energetic materials to form shear bands for a given application of force should correlate well with measured impact sensitivities. To our knowledge, no measurement of this type has been made.

Another possible factor contributing to low-energy impact initiation is that the rate at which energy is transferred from the impact event into vibrational modes of the energetic material influences the onset of chemistry. If we suppose that the shear volume for most crystalline energetic materials is about the same

<sup>®</sup> Abstract published in *Advance ACS Abstracts*, January 1, 1997.



**Figure 3.** Schematic of the load-to-shear process in a crystalline energetic material.

for a given impact event, and that thermal equilibrium is always maintained during the impact event, then sensitivities should track according to decomposition temperatures. This is not the case. Since rates of energy transfer in molecular crystals are sufficiently fast<sup>6</sup> that thermal equilibrium should be maintained throughout a low-energy impact event, in order for energy-transfer rates to play a role in determining impact sensitivity there must be a mechanism that allows for deviations from thermal equilibrium during or immediately following the impact event.

For significant deviation from thermodynamic equilibrium following a perturbation to occur, the perturbation must be faster than those processes that maintain the statistical energy distribution within a molecule or collection of molecules. In crystalline materials, thermal energy initially excites the lowest energy lattice and molecular vibrations and is rapidly equilibrated throughout the full vibrational mode structure of the molecule.<sup>7</sup> Lattice and low-energy molecular vibrations in molecular crystals have frequencies near  $10^{12} \text{ s}^{-1}$ . This means that for the typical impact test mentioned above,  $10^6$  low-energy vibrations occur per microsecond for the duration of the energy transfer from impactor to the affected volume of the explosive. With regard to deviations from thermal equilibrium, energy transfer of 2 J from impactor to explosive occurring over  $1 \mu\text{s}$  is similar to slow heating of the explosive over much longer time scales. The conclusion is that direct coupling of mechanical energy from impactor collision into the vibrational modes of the explosive occurs too slowly to cause significant deviation from thermal equilibrium.

We propose a mechanism that takes the slow impact from the drop weight and directs this energy rapidly into the molecule in a way that leads to significant deviations from thermal equilibrium. In what follows, we develop ideas, based on the Raman spectra of explosive materials, for preferentially redistributing energy from impact into vibrational modes which lead to the onset of chemistry.

### Impact Initiation Model

The first part of the mechanism we propose for impact initiation of a crystalline energetic material involves a load-to-shear event. During a low-velocity impact, a pressure load is created on the crystal. Because the load is not distributed isotropically, at a threshold load pressure the crystal shears (dislocates) along a fracture plane in a way that reduces the pressure load. This is the key to conversion of the slow loading process to a fast process. Essentially, the load buildup causes the crystal to fail (fracture) along a shear plane.<sup>8</sup> This process is illustrated in Figure 3.

For purposes of estimating the shear (dislocation) velocity in molecular crystals, we use the velocity associated with crack growth. For molecular crystals under load, typical values of

crack growth velocity<sup>9</sup> are near  $10^3 \text{ m/s}$ . Velocities of shear (dislocation) bands in the vicinity of the crack decrease rapidly as the distance from the crack front increases.<sup>10</sup> Typical bond lengths<sup>11</sup> in HMX are less than  $2 \times 10^{-10} \text{ m}$ . This means that during crack and associated shear band formation, near the crack front, molecules in adjacent (fracture or shear) planes are moved, relative to each other, a distance of several bond lengths in hundreds of femtoseconds. This dislocation breaks intermolecular bonds associated with phonon modes in the crystal lattice in a time less than one phonon period of vibration. This results in the dislocation "focusing" the impact energy into the phonon modes of the intact material adjacent to the dislocation in a time less than one period of vibration of the modes being excited. This rapid deposition of energy into the phonon modes of the molecule creates a nonequilibrium distribution of energy among the vibrational modes of the molecule.

The second part of the impact initiation mechanism proposed here depends on the vibrational mode structure of the energetic material. It is generally assumed that a molecular solid is a weakly interacting system of individual molecules.<sup>12</sup> Vibrations within the solid are usually divided between phonon states, which are vibrations involving the crystal lattice and may not be ascribed to an individual molecule, and internal vibrational states, which are localized on individual molecules. Because the phonon modes are properties of the crystal lattice, they are often referred to as being delocalized and may be visualized as a "bath" of collective states of the entire solid, which lie lower in energy than the individual molecular internal vibrational states (see Figure 4). When energy is deposited into the phonon modes of the crystal, equilibrium is maintained by the transfer of energy from the phonon modes to the internal vibrational modes. The anharmonic coupling of the phonon modes with the internal molecular vibrations and the excitation of higher lying vibrational modes is often termed "vibrational up-pumping". Extensive investigations into this phenomenon have been made by Dlott et al.<sup>13</sup>

In our model, we postulate that the initial excitation (from the shear (dislocation) event) is instantaneously distributed, according to Boltzmann statistics, among the phonon modes and those low-lying vibrational modes with fundamental energies of less than  $250 \text{ cm}^{-1}$ . This cutoff value was chosen as the maximum value of a fundamental vibration which is highly coupled to the phonon "bath" of the bulk, since phonon densities of states for the energetic materials examined in this report reach a maximum (room temperature) near  $100 \text{ cm}^{-1}$ . Overtones of these low-lying vibrational modes are also populated. Higher energy fundamental internal vibrational energy levels are not affected by the initial perturbation, since the perturbation occurs on a time scale faster than a period of vibration of the phonon modes excited by the initial shear-dislocation event.

Impact sensitivity is determined by how fast energy is transferred from this initially excited group of states, which we call the "phonon manifold", to internal vibrational states with fundamental vibrational energies up to  $700 \text{ cm}^{-1}$  ("internal vibrational manifold"). This upper limit cutoff value was chosen because previous work<sup>14</sup> has indicated that energy transfer into vibrational modes between  $400$  and  $600 \text{ cm}^{-1}$  may be rate determining for shock-induced initiation. We propose that the rate of this energy transfer is governed by Fermi's Golden Rule,<sup>15</sup> which states that energy transfer is most efficient for resonant processes. Off-resonance energy transfer is a function of the product of the optical line width of the state being excited and the phonon density of states. Materials that transfer energy to the "internal vibrational manifold" fastest are most sensitive because a greater fraction of the initial energy goes into vibrational modes which may lead to bond breaking, instead of

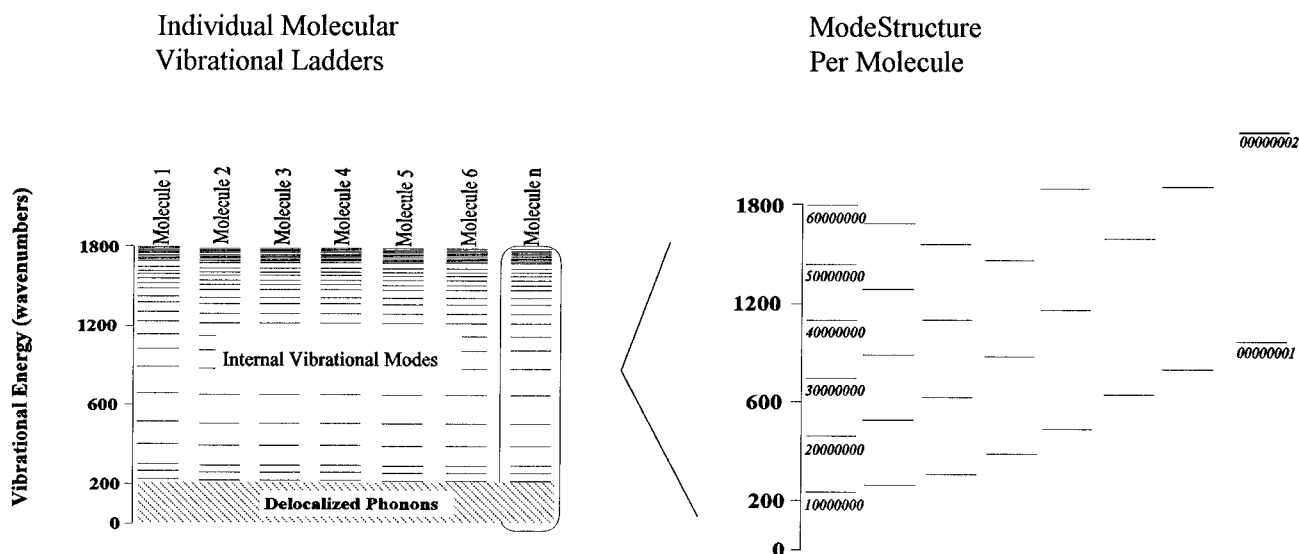


Figure 4. Vibrational structure of the bulk solid (left) and of an individual molecular constituent of the bulk solid (right).

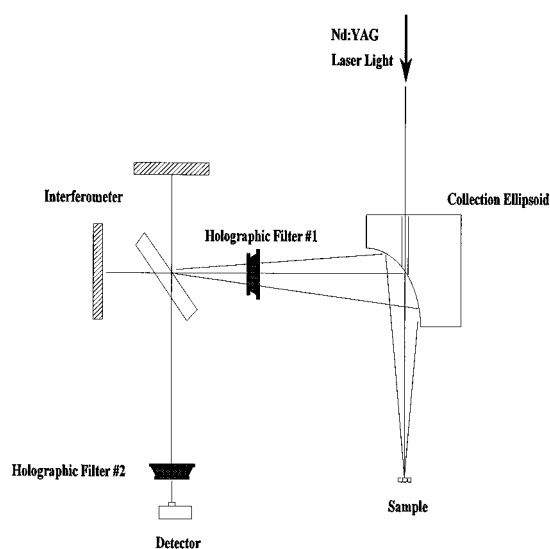


Figure 5. Simple diagram of the experimental apparatus used in these experiments.

being distributed among the phonon "bath" of the bulk material. Finally, we use measured Raman spectra to construct energy level diagrams, using a harmonic oscillator approximation, for several explosive materials, and obtain a quantitative measure of impact sensitivity using an energy-transfer model based on the ideas outlined above.

### Experimental Section

The experimental apparatus has been described previously.<sup>16</sup> Briefly, the equipment employed in these experiments consists of a Bomem DA-8.02 Fourier transform infrared spectrometer, to which a Raman accessory has been added. Incident laser radiation is provided by a Quantronix Series 100 Nd:YAG laser. A simple sketch of the experimental apparatus is shown in Figure 5. Raman-shifted radiation is collected using a back-scattering geometry and is detected, after filtering and interferometer modulation, using a liquid nitrogen-cooled InGaAs detector. All spectra reported here were measured at 4  $\text{cm}^{-1}$  resolution using coaddition of 256 scans. The incident laser power at the sample was 400 mW. Neat samples (typically white or yellow powders) of energetic materials were placed in 1 mm i.d. glass capillary tubes, and the Nd:YAG laser focused (spot size approximately 0.5 mm diameter) on the surface of the tube. A near-infrared viewing scope (FJW Optical Systems)

was used to visually check laser alignment and also to ensure that the back-scattered radiation was brought to a tight focus at the entrance aperture of the spectrometer. No correction was made to any of the spectra to account for responsivity of the detector, interferometer, or filters used in the experiments. All energetic materials used in these experiments were obtained from in-house sources.

### Background

In calculations to determine impact sensitivity, we use Raman spectra to construct an energy level diagram for the solid explosives used in this study. We use Raman spectroscopy because measurements are well resolved, rapid, in situ, and nondestructive and have been proven useful in the characterization of explosives.<sup>16</sup> Because energies of vibrational levels are required for the calculations performed here, the best approach is to use values of energies of vibrational levels from a normal-mode analysis of each material under consideration. Unfortunately, calculations for most energetic materials have yet to be performed, especially those calculations that include lattice perturbations to the internal vibrations. Additionally, application of the theory outlined here on an unknown material cannot rely on information obtained using a normal-mode analysis. Also, symmetry exclusions<sup>17</sup> prevent Raman spectroscopy from measuring all internal fundamental vibrational transitions.

As a measure of the error which might be caused by using a Raman spectrum to construct a vibrational energy level diagram for an energetic material, a density functional theory calculation for a single molecule of RDX was performed.<sup>18</sup> Table 1 shows a comparison, from 100 to 700  $\text{cm}^{-1}$ , of calculated and observed (using Raman spectroscopy) vibrational frequencies for RDX. Although the agreement between observed and calculated values shown in Table 1 is good, the agreement probably would have been better if perturbations from the crystal lattice were included in the calculation. Agreement at higher frequencies (not shown) was always within a few percent of the calculated value. Agreement between all observed and calculated values, with one exception, is always less than 6%, with the one exception by 9%. We believe that the three frequencies not predicted by the calculation are due to lattice modes (149, 168  $\text{cm}^{-1}$ ) or to lattice mode—internal mode coupling (487  $\text{cm}^{-1}$ ). Of the 14 calculated modes between 100 and 700  $\text{cm}^{-1}$ , 11 were observed in the Raman spectrum, although one mode, calculated at 438  $\text{cm}^{-1}$ , was obscured by shoulders, in the measured spectrum, from adjacent peaks.

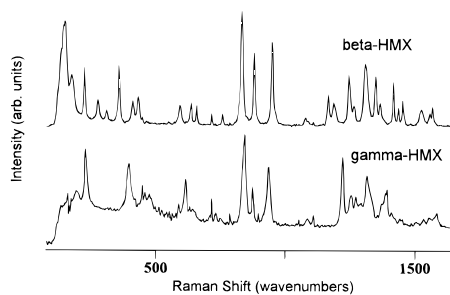


**Figure 6.** FT Raman spectra of  $\beta$ -HMX and of  $\gamma$ -HMX. The signal-to-noise ratio in the spectrum of  $\gamma$ -HMX is lower than that of  $\beta$ -HMX, partially due to the lower density of  $\gamma$ -HMX.

**TABLE 1: Comparison of Measured Raman Shift Frequencies for Neat RDX and a Density Functional Theory Calculation for a Single Molecule of RDX**

obsd Raman shift ( $\text{cm}^{-1}$ )	calcd vibrational frequency ( $\text{cm}^{-1}$ )/intensity (KM/mol)
109	107/0.0074
149	
168	
206	209/8.3177
225	229/1.7658
346	325/2.5840
385	371/0.0752
415	403/8.5605
	405/0.6307
obscured	438/5.8478
462	463/25.9101
487	
546	579/10.1865
590	588/0.3703
605	609/14.5462
	651/0.6618
668	676

As an example of the application of the proposed theory, we examine impact initiation in two of the polymorphs of HMX. HMX (octahydro-1,3,5,7-tetranitro-1,3,5,7-tetrazocine) is an important energetic material used in explosives and propellant formulations. HMX is known to exist in the solid state in four polymorphic forms, referred to as  $\alpha$ -,  $\beta$ -,  $\gamma$ -, and  $\delta$ -HMX.<sup>19</sup> Figure 6 shows the Raman spectrum of  $\beta$ - and  $\gamma$ -HMX shifted from 200 to 1600  $\text{cm}^{-1}$  relative to the laser line. The spectra are not superimposable, with the most apparent differences in peak position occurring at small Raman shifts.  $\beta$ -HMX is the most commonly encountered form of HMX and is more thermally stable than  $\gamma$ -HMX.  $\beta$ -HMX exists in the “chair” configuration, giving the molecule a center of symmetry, while  $\gamma$ -HMX exists in a “boat” configuration.  $\beta$ - and  $\gamma$ -HMX are well suited for studies of impact initiation since they differ markedly in their impact sensitivity.<sup>20</sup>  $\beta$ -HMX is less sensitive and has an impact sensitivity in the midrange of most secondary explosive materials (similar to RDX). On the other hand,  $\gamma$ -HMX has an impact sensitivity more like a primary explosive (similar to Pb styphnate).  $\gamma$ -HMX may be quantitatively prepared from  $\beta$ -HMX by a safe and simple method.<sup>20</sup>

### Qualitative Evaluation of Impact Sensitivities

In accordance with the previous discussion, Figures 7 and 8 are energy level diagrams, constructed using the spectra shown in Figure 6, of vibrational levels for  $\beta$ -HMX and  $\gamma$ -HMX up to 700  $\text{cm}^{-1}$ . Since intramode vibrational energy transfer is assumed to be rapid,<sup>21</sup> overtone vibrational levels are included for each transition measured in the spectra. This is an essential feature of the model presented here. Overtone energy levels are assumed to be integral multiples of energies of Raman spectral features below 250  $\text{cm}^{-1}$  shift. By assuming that

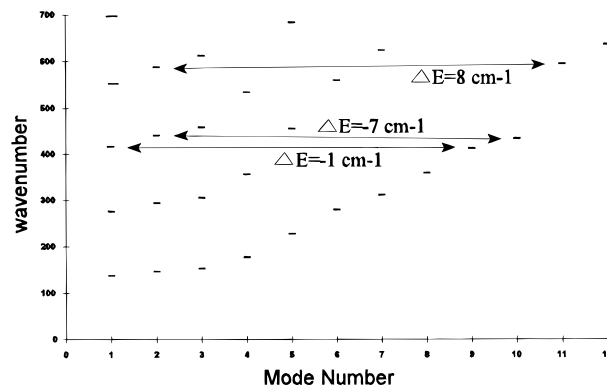


**Figure 7.** Energy level diagram for  $\beta$ -HMX constructed from the spectrum shown in Figure 6. Arrows indicate transitions from the phonon manifold to the internal vibration manifold for which the energy mismatch is less than 10  $\text{cm}^{-1}$ . Impact test results indicate  $\beta$ -HMX to be less sensitive than  $\gamma$ -HMX.

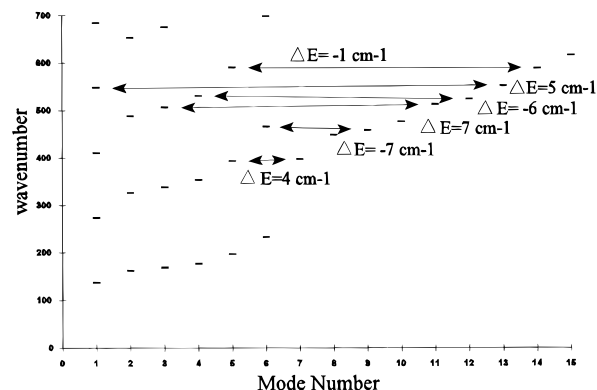


**Figure 8.** Energy level diagram for  $\gamma$ -HMX constructed from the spectrum in Figure 6. Arrows indicate transitions from the phonon manifold to the internal vibration manifold for which the energy mismatch is less than 10  $\text{cm}^{-1}$ . Impact test results indicate  $\gamma$ -HMX to be more sensitive than  $\beta$ -HMX.

overtone levels are harmonic with the fundamental, we are assuming that energy transfer from a third overtone level is identical with energy transfer involving four quanta of the fundamental. As previously mentioned, it was assumed that the rate-limiting step for impact-induced chemical reaction involves transfer of energy from the “phonon manifold” to “internal vibration manifold” modes having fundamental energies between 400 and 700  $\text{cm}^{-1}$ . Previous studies<sup>14</sup> have reported a correlation between impact sensitivities and densities of states over this region of the spectrum for several energetic materials. Additionally, intramode energy transfer at energies above these values is believed to occur fast enough so that quasiequilibrium is always maintained among higher energy states.<sup>22</sup>

We propose that the rate of energy transfer from overtones (or equivalently, multiphoton transitions) of “phonon manifold” molecular vibrations to fundamental vibrations belonging to the “internal vibration manifold” plays a role in determining impact sensitivity. These energy transfer processes are assumed to be most efficient when the energy mismatch between donor and acceptor states is minimized. In addition, energy transfer is most favored when the total quantum number change which accompanies the process is minimized.<sup>23</sup> Figures 7 and 8 show that the number of energy-transfer processes originating from the “phonon manifold” which have small energy mismatches (arbitrarily chosen as  $\Delta E < 10 \text{ cm}^{-1}$ ) for transitions that excite fundamental vibrations between 400 and 700  $\text{cm}^{-1}$  in  $\gamma$ -HMX is double that for  $\beta$ -HMX. This suggests that  $\gamma$ -HMX should be the more impact sensitive of the two polymorphs, in agreement with experiment.

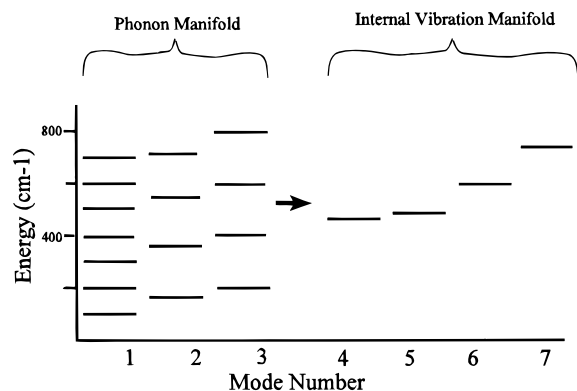


**Figure 9.** Division of vibrational energy levels within a molecule into phonon and internal vibration manifolds. Following perturbation by impact, energy is transferred from the phonon manifold to the internal vibration manifold.

### Energy-Transfer Model

To obtain a quantitative measure of impact sensitivity from measured vibrational frequencies of the crystalline and polycrystalline explosive samples analyzed in this report, it was necessary to construct a numerical model which describes energy redistribution in the solid following a perturbation. The framework of that model is described in what follows.

As postulated previously, energy from the shear-dislocation event is deposited into the phonon modes and those low-lying internal molecular vibrational modes which have fundamental vibrational energies very near to, or within the phonon energy "bath". For this study, it was assumed that internal molecular vibrations with fundamental vibrational frequencies less than  $250\text{ cm}^{-1}$  are strongly coupled to the phonon modes and that the initial perturbation (shear-dislocation event) excites these low-lying internal vibrational modes, and their overtones, at the same rate at which the phonon modes are excited. It should be emphasized that this assumption is a main difference between the theory as described here, and previous theories of vibrational up pumping.<sup>7</sup>

In our model, the energy from the initial perturbation is instantaneously distributed among the energy levels of the "phonon manifold" according to Boltzmann statistics, while the vibrational energy levels outside of the "phonon manifold" remain unaffected. As discussed previously, this occurs because the excitation from the shear-dislocation event is faster than most relaxation processes in the solid. Following the initial, fast perturbation, energy redistribution takes place from the "phonon manifold" to the "internal vibrational manifold". Vibrational energy transfer can occur between all levels contained in the model. It should be emphasized that since the initial perturbation is distributed among the energy levels within the "phonon manifold" according to Boltzmann statistics, energy transfer from overtones of fundamental vibrations becomes important. The model essentially simulates microscopic energy transfer between two thermal baths. Sensitivity is determined by the rate at which energy is transferred from the initially excited "phonon manifold" to the "internal vibrational manifold". This process is shown in Figure 9.

The model employed to describe energy transfer is a simple hybrid of previous theories which have been used with success to describe vibrational energy transfer in gases<sup>15</sup> and vibrational up pumping in solids.<sup>7</sup> The main idea is that the predominant pathway of energy randomization following a fast perturbation is intramolecular. That is, energy is transferred from one state of a molecule to another state of the same molecule. Impact-sensitive materials transfer energy into higher energy fundamentals faster than less sensitive materials. The initially

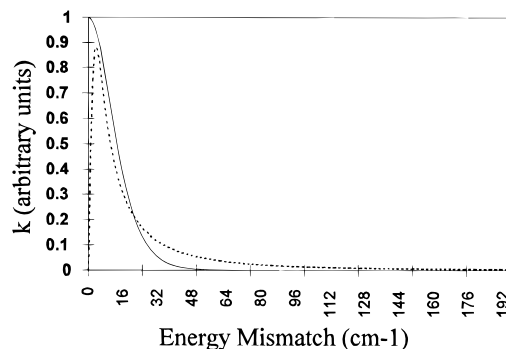


**Figure 10.** Dependence of the unimolecular rate constant on energy mismatch  $\Delta E$  for vibrational intramolecular energy transfer. Dashed line is the product of a Lorentzian lineshape ( $\text{hwhm} = 5\text{ cm}^{-1}$ ) and an approximation to the density of states typical to crystalline explosive materials. The smooth line is the function used in the calculations reported in this paper.

nonstatistical ensemble of excited molecules eventually reaches a distribution described by Boltzmann statistics.

For the model developed here, the vibrational energy-transfer rate kinetics are unimolecular. The rate of energy transfer is dependent on the energy mismatch between the two vibrational levels exchanging energy, whether the transfer is intramode or intermode (intramode is favored), and the total quantum number change for the transfer (small changes are favored). These conventions are in keeping with standard theories of vibrational energy transfer in condensed phases and in gases.<sup>15</sup>

The first-order rate constant used to describe energy transfer between vibrational levels in the solid is a function of the transfer energy mismatch  $\Delta E = E_i - E_j$ , where  $E_i$  is the energy of the state initially excited, and  $E_j$  is the state to which energy is transferred, and the temperature,  $T$ , of the system. We have chosen the dependence of the rate constant on the transfer energy mismatch to be proportional to  $\text{sech}^2(\Delta E/kT)$ , in accordance with simple treatments of near-resonant energy transfer in gases.<sup>24</sup> A difference between the function employed here to describe rate constant dependence on energy mismatch and that used for gas phase work is as follows. For gas-phase vibrational energy transfer, energy mismatch must be made up by rotations, for which the density of states is near a maximum near zero energy. However, for solid-phase transitions, energy mismatch must be made up by phonons, for which the density of states is typically peaked<sup>14</sup> near  $100\text{ cm}^{-1}$ . A reasonable function to use for solid-state calculations is the product of the density of states function with a function which describes the optical width of the vibrational energy transition. The resulting function is zero near zero energy mismatch and is slightly broader than the optical line width (see Figure 10). For calculations employed here, an approximation to this product function is used (see Figure 10) which is peaked near zero energy mismatch, in accordance with Fermi's Golden Rule. Additionally, inclusion of resonant energy processes implicitly takes into account higher order phonon processes. All transition rate constants are first calculated in the exothermic direction, and microscopic reversibility is used to calculate the rate constant for the endothermic process. When there is an energy mismatch,  $\Delta E$ , accompanying energy transfer, energy must be taken up by or supplied by the bulk sample. When this happens, heating and cooling of the sample occur, changing the equilibrium population distributions. The inclusion of heating is necessary for proper performance of the model.

The calculation of the time dependence of vibrational level populations following perturbation divides the populations in each level into an equilibrium part,  $N_i^e$ , and a perturbation part  $n_i$ , where the subscript  $i$  refers to the level in question. It may

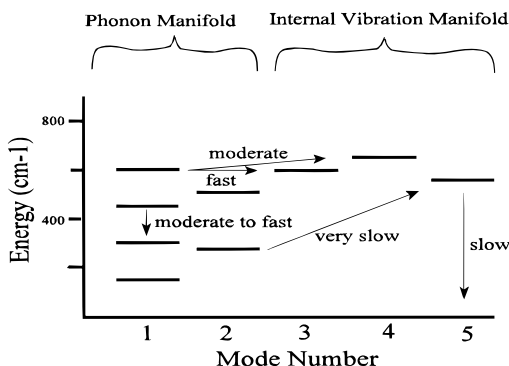


**Figure 11.** The 10-level system used to test the model for vibrational energy transfer in solids. Arrows indicate relative rates, based on energy mismatch,  $\Delta E$ , for several transitions.

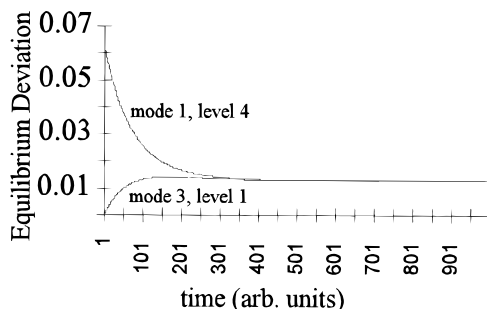


**Figure 12.** Changes in deviation from equilibrium population, following an initial perturbation, for a phonon manifold level (mode 1, level 4, in Figure 11) and an internal vibration manifold level (mode 3, level 1, in Figure 11). The two levels have similar energies ( $\Delta E < 5 \text{ cm}^{-1}$ ).

be shown<sup>25</sup> that for first-order rate processes in multilevel systems, the change in the deviation from equilibrium population of level  $J$  is approximated by

$$\Delta n_J = \left\{ \sum_{I \neq J} [K_{IJ} n_I] - \sum_{I \neq J} [K_{JI} n_J] \right\} \Delta t \quad (1)$$

where the sum is over all levels (except  $I = J$ ),  $K_{IJ}$  and  $K_{JI}$  are forward and reverse rate constants,  $n_I$  and  $n_J$  are deviation from equilibrium population of levels  $I$  and  $J$ , respectively, and  $\Delta t$  is the time increment. The change in temperature,  $\Delta T$ , over the same time interval is given by

$$\Delta T = \sum_I (n_I(t) - n_I(t-1)) E_I / C_{PI} \quad (2)$$

where the sum is over all levels,  $n_I(t)$  and  $n_I(t-1)$  are population deviations from equilibrium separated by one time element,  $E_I$  is the energy of level  $I$ , and  $C_{PI}$  is the vibrational contribution to the heat capacity of level  $I$ .

Figure 11 shows the vibrational energy level structure for a synthetic 10-level molecule used to test the model for vibrational energy transfer outlined above. Shown in Figure 11 are relative rates of energy transfer for different transitions, where the rate of each transition is dependent upon energy mismatch,  $\Delta E$ , for the transition being considered.

Figure 12 shows results of calculations, using the model just described, of changes in vibrational level population deviations from equilibrium for the energy level system in Figure 11, following a perturbation of the phonon modes equivalent to raising the "phonon manifold" temperature to 1000 K. The two levels, from Figure 11, shown in Figure 12 are the highest energy excited "phonon manifold" level (mode 1, level 4), and the "internal vibration manifold" level with energy closest to this "phonon manifold" level (mode 3, level 1). Since these

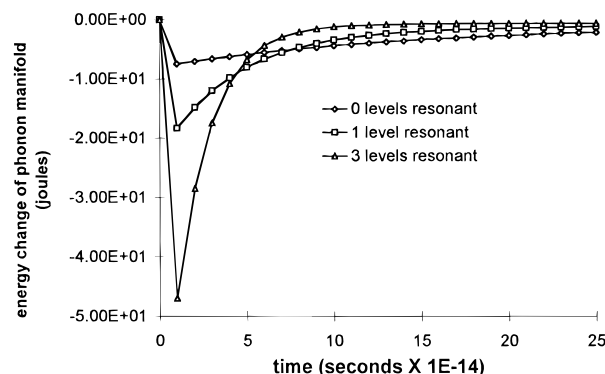


**Figure 13.** Change in phonon manifold energy (joules) as a function of time after perturbation, for 10-level systems which differ in the number of levels with favorable energy mismatch,  $\Delta E$ , between phonon manifold energy levels and energy levels within the internal vibration manifold. The rate constant for resonant intramolecular energy transfer is taken to be  $1 \times 10^{13} \text{ s}^{-1}$  (see text).

two levels are similar in energy, they equilibrate quickly and then, as a coupled pair, equilibrate with the remainder of the energy levels in the model system. Since the initial perturbation supplied energy to the model system, the new equilibrium level is caused by the overall increase in system temperature.

Recently, Fried and Ruggiero<sup>14</sup> have calculated rates of upconversion from phonon modes to internal vibrational modes. Rates of energy transfer from phonon modes to internal vibrational modes are calculated as a function of the density of states which may contribute energy during the upconversion process. Since optical measurements of intensities of vibrational transitions yield information on the density of states only for  $k \sim 0$  (a limitation when using Raman spectroscopy), Fried and Ruggiero use neutron-scattering data to estimate densities of states. The authors then calculate rates of energy transfer from phonon modes into internal vibrational modes which are deemed likely to lead to the onset of reaction (e.g., vibration of the N–N bond in a nitramine). A good correlation is shown between rates of energy transfer from phonon modes to particular frequencies that may lead to onset of reaction.

We have chosen a slightly different approach for several reasons. First, we wished to incorporate our model for low-energy impact initiation by shear/dislocation with an easily accessible diagnostic such as Raman spectroscopy. Second, our model supposes that the phonon modes maintain equilibrium among themselves throughout the upconversion process and that the relaxation process involves equilibration of two energy baths, one composed of the phonon modes, and one composed of the internal vibrational energy modes. Also, we believe that the overall internal vibrational mode temperature is rate determining, since at higher energies the internal vibrational modes equilibrate rapidly. Therefore, relating single-mode internal vibrational mode temperatures to impact sensitivities may be misleading.

Figure 13 shows the change in energy of the "phonon manifold" as a function of time after initial perturbation, for the 10-level system described above. The three curves represent vibrational level systems that are identical, except that they differ slightly in the energies of the vibrational levels which make up the "internal vibration manifold". The three systems have three, one (shown in Figure 11), or zero "internal vibration manifold" energy levels within  $10 \text{ cm}^{-1}$  of a "phonon manifold" energy level. The energy level structures of the three systems are shown in Table 2.

Figure 13 shows that for the model 10-level vibration system presented above, the change in energy of the "phonon manifold", at times immediately following the initial perturbation, is

**TABLE 2: Vibrational Energies ( $\text{cm}^{-1}$ ) of Levels That Make up the Three 10-Level Systems Shown in Figure 13<sup>a</sup>**

system 1 level energies 3 transitions $\Delta E < 10 \text{ cm}^{-1}$					system 2 level energies 1 transition $\Delta E < 10 \text{ cm}^{-1}$					system 3 level energies 0 transitions $\Delta E < 10 \text{ cm}^{-1}$				
150	280	600	601	602	150	280	600	625	640	150	280	580	625	640
300	560				300	560				300	560			
450					450					450				
600					600					600				

<sup>a</sup> The first two columns in each distribution belong to the phonon manifold. The last three columns in each distribution belong to the internal vibration manifold.

**TABLE 3: The Seven Explosive Samples Analyzed in This Report and Experimentally Determined Impact Sensitivities**

explosive material	impact sensitivity <sup>27</sup> (N m)	calculated change in phonon energy for first 10 fs following shear dislocation (J)
PETN (pentaerythrol tetranitrate)	3	-50.43
$\gamma$ -HMX ( $\gamma$ -cyclotetramethylenetetranitramine)	est 3	-51.51
$\beta$ -HMX ( $\beta$ -cyclotetramethylenetetranitramine)	7.4	-40.35
RDX (cyclo-1,3,5-trimethylene-2,4,6-trinitramine)	7.4	-46.85
TNT (trinitrotoluene)	15	-35.67
TATB (triaminotrinitrobenzene)	>49	-9.25

dependent upon the number of near resonant energy transfer pathways from the “phonon manifold” to the “internal vibration manifold”.

## Results and Discussion

To extend the model described above to evaluation of real explosive samples, energy level diagrams, from measured Raman spectra,<sup>26</sup> were constructed for the neat explosives PETN,  $\beta$ -HMX,  $\gamma$ -HMX, TATB, nitroguanidine, RDX, and TNT. Table 3 shows the chemical name for each compound examined in this test and experimentally determined (drop weight test) impact sensitivities.<sup>27</sup> To generate the energy levels used as input to the model calculation, a commercial software peak picking routine (Grams 386, Galactic Industries) was used to select all Raman spectral features between 100 and  $700 \text{ cm}^{-1}$  for each of the explosive samples. Each peak selected was assumed to belong to a different mode of internal vibration in the molecule. For each peak measured with an energy less than  $350 \text{ cm}^{-1}$ , an overtone was generated by multiplying the energy of that peak by integral values, such that overtones up to  $700 \text{ cm}^{-1}$  were included as input to the model calculation. By this convention, a single spectral peak measured at  $100 \text{ cm}^{-1}$  would have six overtone levels considered in the calculation.

Once the energy level diagram was constructed, all modes with fundamentals less than  $250 \text{ cm}^{-1}$  were considered as part of the “phonon manifold”, with all other modes belonging to the “internal vibration manifold”. The initial perturbation then excited all modes with fundamentals less than  $250 \text{ cm}^{-1}$ , and the overtones associated with each of those modes. The excitation was distributed among these fundamental and overtone levels according to the Boltzmann distribution. The excitation used was an initial heating of the phonon manifold to 1000 K. Several other, lesser degrees of heating were tried to see if the degree of initial excitation affected the behavior of the model. In each case, the output of the model was independent of the magnitude of the initial excitation, as expected since first-order kinetics are employed in the model.

The first-order intramolecular energy-transfer rate constant for resonant processes was approximated in the following manner. Measurements<sup>15</sup> of vibrational relaxation of diatomic molecules in inert-gas matrixes have shown the first-order rate constant for processes with an energy mismatch,  $\Delta E$ , near  $100 \text{ cm}^{-1}$  to be on the order of  $1 \times 10^{10} \text{ s}^{-1}$ . For this work we have chosen the dependence of the rate constant on the transfer energy mismatch to be proportional to  $\text{sech}^2(\Delta E/kT)$ . Using this function, an energy-transfer process with an energy mismatch of  $100 \text{ cm}^{-1}$  would have a resonant ( $\Delta E = 0$ ) energy-

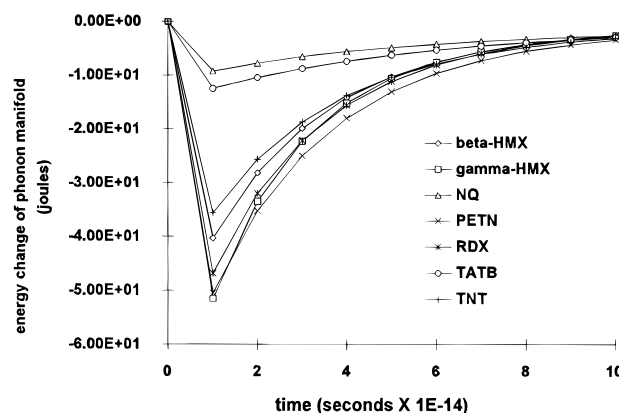


**Figure 14.** Change in phonon manifold energy (joules) as a function of time after perturbation for the seven explosive materials examined in this report. The rate constant for resonant intramolecular energy transfer is taken to be  $1 \times 10^{13} \text{ s}^{-1}$  (see text).

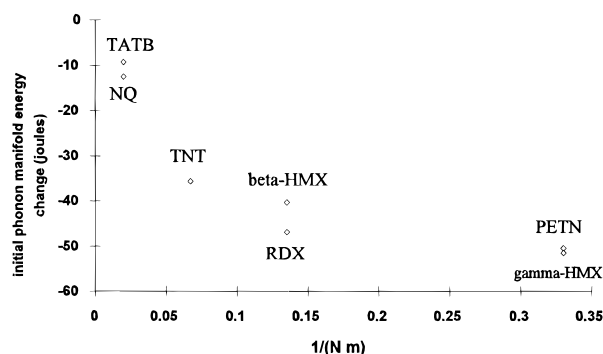


**Figure 15.** Experimentally measured impact sensitivities plotted against the initial change (first 100 fs) in energy of the phonon manifold following the shear dislocation.

transfer rate constant of  $1 \times 10^{13} \text{ s}^{-1}$ . This value for the first-order rate constant for resonant energy-transfer processes was used throughout the calculations reported here.

Figure 14 shows the change in “phonon manifold” energy as a function of time after initial perturbation, for the seven explosive materials examined for this report. Figure 15 shows a plot of “phonon manifold” energy change during the first 10 fs following the perturbation, calculated using the model developed here, versus experimentally determined impact sensitivities. The calculated differences between very sensitive (PETN,  $\gamma$ -HMX) and sensitive (RDX,  $\beta$ -HMX) are small, with the differences between the sensitive materials and insensitive materials (TATB, nitroguanidine) much larger. The correlation

between results of impact tests for these explosives and calculated rates of energy transfer from the "phonon manifold" of each of the explosives is good. We should note that TATB and nitroguanidine are among the most insensitive of all explosives, and the reported impact sensitivities for these compounds varies in the literature. We chose to use values reported in one of the most used references,<sup>27</sup> which reported an impact sensitivity for TATB of 50 N m and reported "no reaction up to 49 N m" for nitroguanidine.

Figure 14 shows that for each of the explosive samples examined in this report, the energy transferred from the "phonon manifold" reaches at least half of its initial value in less than 50 fs. During the shear-dislocation event, only a small fraction of the bulk sample is actually perturbed, with phonons dissipating heat rapidly throughout the bulk material. Phonons travel at approximately the speed of sound in solid materials (generally on the order of several micrometers per nanosecond<sup>28</sup>). Therefore, for the model reported here, dissipation of energy from the phonon manifold to the bulk of the material is much slower than energy transfer from the "phonon manifold" to the "internal vibration manifold".

There seems to be general agreement that many different physical properties and processes occurring within the solid phase contribute to impact sensitivity.<sup>29</sup> We believe these results show that the number of near-resonant energy-transfer processes which can result in energy transfer between the "phonon manifold" and the "internal vibration manifold" of a crystalline explosive material influences low-energy impact sensitivity. These results support the importance of shear-dislocation effects in molecular crystals, allowing a slow event (impact) to rapidly channel energy into specific vibrational modes of the molecule.

The model has several shortcomings, chief among which are that we have not accounted for anharmonicity of vibrational levels, have neglected transition intensities, and have not considered orthogonality of eigenvectors of vibrations in calculating energy-transfer rates. We hope to be able to address these limitations in the near future. Additionally, we have not mentioned effect of particle size on sensitivity, although current work in our lab (not presented here) shows correlation between model calculations and impact testing of RDX of particle sizes from 38  $\mu\text{m}$  to several millimeters. Several ways to improve and check the theory are currently being explored. These include calculations of how the lattice perturbs the individual molecule, inclusion of degeneracies, and transition intensities in the rate calculations (not included in the current model), inclusion of combination (i.e., three state) transitions, and refinement of the calculation of rate coefficients for near-resonant energy transfer in condensed media. However, even given the shortcomings of the current model, the success of the theory outlined above in determining impact sensitivities from room-temperature measurements of Raman spectra of crystalline explosives merits further consideration.

## Conclusion

A new mechanism which contributes to the determination of low-energy impact initiation of crystalline energetic materials, based upon transition of a slow event (impact) into a fast event (shear-dislocation), is proposed. The effect of the shear-dislocation event is to deposit energy into a band of molecules adjacent to the shear-dislocation planes faster than energy redistribution processes can randomize that energy. Following this rapid, exclusive perturbation of low-energy modes, the initial

rate of energy transfer from these low-energy modes into states with higher energy is determined by Fermi's Golden Rule. Results of calculations suggest that this initial rate of energy transfer, from states within a low-energy "phonon manifold" to states within a higher energy "internal vibrational manifold", plays a role in determining impact sensitivities of the explosives examined in this report.

**Acknowledgment.** The authors wish to thank Prof. Dana Dlott for a critical review of the manuscript and for several helpful discussions which corrected several errors in the original manuscript. The authors would also like to thank Drs. Betsy Rice and Martin Miller of ARL and Sam Trevino of NIST for helpful discussions on the subject matter presented in the paper.

## References and Notes

- (1) Robertson, R. *Trans. Chem. Soc.* **1921**, 18.
- (2) Coffey, C. S.; DeVost, V. F. *Propellants, Explos., Pyrotechn.* **1995**, 20, 105.
- (3) *CPIA/M3 Solid Propellant Ingredients Manual*; Chemical Propulsion Information Agency, The Johns Hopkins University, Columbia, MD, Sept 1994.
- (4) Coffey, C. S. Initiation of Crystalline Explosives by Shock or Impact. In *Decomposition, Combustion, and Detonation Chemistry of Energetic Materials*; Material Research Society Symposium Proceedings; Materials Research Society: Pittsburgh, PA, 1996; Vol. 418, pp 331–336.
- (5) Dick, J. J. *App. Phys. Lett.* **1984**, 44, 859.
- (6) Hong, X.; Hill, J. R.; Dlott, D. D. Vibrational Energy Transfer in High Explosives: Nitromethane. In *Decomposition, Combustion, and Detonation Chemistry of Energetic Materials*; Material Research Society Symposium Proceedings; Materials Research Society: Pittsburgh, PA, 1996; Vol. 418, pp 357–362.
- (7) Dlott, D. D.; Fayer, M. D. *J. Chem. Phys.* **1990**, 92, 3798.
- (8) Coffey, C. S.; Jacobs, S. J. *J. Appl. Phys.* **1981**, 52, 6991.
- (9) Gazonas, G. A. *Mech. Mater.* **1993**, 15, 323.
- (10) Sharma, J.; Coffey, C. S.; Ramaswamy, A. L.; Armstrong, R. W. Atomic Force Microscopy of Hot Spot Reaction Sites in Impacted RDX and Laser Heated AP. In *Decomposition, Combustion, and Detonation Chemistry of Energetic Materials*; Material Research Society Symposium Proceedings; Materials Research Society: Pittsburgh, PA, 1996; Vol. 418, pp 257–266.
- (11) Pauling, L. *The Nature of the Chemical Bond*; Cornell University Press: Ithaca, NY, 1960.
- (12) Kitaigorodskii, A. I. *Molecular Crystals and Molecules*; Academic Press: New York, 1973.
- (13) Chen, S.; Tolbert, W. A.; Dlott, D. D. *J. Phys. Chem.* **1994**, 98, 7759. Also see: Tokmakoff, A.; Fayer, M. D.; Dlott, D. D. *J. Phys. Chem.* **1993**, 97, 1901 and references therein.
- (14) Fried, L. E.; Ruggiero, A. J. *J. Phys. Chem.* **1994**, 98, 9786.
- (15) Yardley, J. T. *Introduction to Molecular Energy Transfer*; Academic Press: New York, 1980.
- (16) McNesby, K. L.; Wolfe, J. E.; Morris, J. B.; Pesce-Rodriguez, R. A. *J. Raman Spectrosc.* **1994**, 25, 75.
- (17) Herzberg, G. *Infrared and Raman Spectra of Polyatomic Molecules*; Van Nostrand Reinhold Co.: New York, 1966.
- (18) Rice, B. Army Research Lab, private communication.
- (19) Goetz, F.; Brill, T. B. *J. Phys. Chem.* **1979**, 83, 340.
- (20) Cady, H. H.; Smith, L. C. Studies on the Polymorphs of HMX; LAMS-2652; Los Alamos Scientific Laboratory Reports, 1962.
- (21) Shamah, I.; Flynn, G. *J. Chem. Phys.* **1978**, 69, 2474.
- (22) Chen, S.; Tolbert, W. A.; Dlott, D. D. *J. Phys. Chem.* **1994**, 98, 7759.
- (23) Schwartz, R. N.; Slawsky, Z. I.; Herzfeld, K. F. *J. Chem. Phys.* **1952**, 20, 1591.
- (24) Rapp, D. *J. Chem. Phys.* **1965**, 43, 316.
- (25) Zittel, P. F.; Moore, C. B. *J. Chem. Phys.* **1973**, 58, 2004.
- (26) Fell, N. F.; McNesby, K. L. *J. Raman Spectrosc.*, in press.
- (27) Meyer, R. *Explosives*; Verlag Chemie: New York, 1977.
- (28) *CRC Handbook of Chemistry and Physics*, 66th ed.; Weast, R. C., Ed.; CRC Press Inc.: Boca Raton, FL, 1986.
- (29) *Decomposition, Combustion, and Detonation Chemistry of Energetic Materials*; Material Research Society Symposium Proceedings; Brill, T. B., Russell, T. B., Tao, W. C., Wardle, R. B., Eds.; Materials Research Society: Pittsburgh, PA, 1996; Vol. 418.